Multilayered Al/CuO thermite formation by reactive magnetron sputtering: Nano versus micro

Marine Petrantoni, Carole Rossi, Ludovic Salvagnac, Véronique Conédéra, Alain Estève, Christophe Tenailleau, Pierre Alphonse, Yves J. Chabal

Multilayered Al/CuO thermite formation by reactive magnetron sputtering: Nano versus micro

M. Petrantoni,[1,2,a)] C. Rossi,[1,2] L. Salvagnac,[1,2] V. Conédéra,[1,2] A. Estève,[1,2] C. Tenailleau,[2,3] P. Alphonse,[3] and Y. J. Chabal[4]
[1]*CNRS–LAAS, 7 Avenue du Colonel Roche, F-31077 Toulouse, France*
[2]*UPS, INSA, INP, ISAE, LAAS, Université de Toulouse, F-31077 Toulouse, France*
[3]*CIRIMAT, 118 route de Narbonne, 31062 Toulouse Cedex 04, France*
[4]*Department of Materials Science and Engineering, University of Texas at Dallas, 800 W. Campbell Rd., RL 10 Richardson, Texas 75080, USA*

Multilayered Al/CuO thermite was deposited by a dc reactive magnetron sputtering method. Pure Al and Cu targets were used in argon–oxygen gas mixture plasma and with an oxygen partial pressure of 0.13 Pa. The process was designed to produce low stress (<50 MPa) multilayered nanoenergetic material, each layer being in the range of tens nanometer to one micron. The reaction temperature and heat of reaction were measured using differential scanning calorimetry and thermal analysis to compare nanostructured layered materials to microstructured materials. For the nanostructured multilayers, all the energy is released before the Al melting point. In the case of the microstructured samples at least 2/3 of the energy is released at higher temperatures, between 1036 and 1356 K.

I. INTRODUCTION

The use of modern thin film deposition techniques for the fabrication and integration of nanoenergetic material on functional substrates is being considered to produce micropower sources on an electronic chip. The potential applications of "nanoenergetics-on-a-chip" systems are wide and include micropropulsion, vehicles with nanoairbags, nanofluidic, and nanorocket, nanofuze.[1–6] Among thermite materials, Al/CuO is interesting for nanoenergetics-on-a-chip because Al and CuO are commonly used in microelectromechanical systems (MEMS) and their reaction is highly exothermic. Integration of Al/CuO_x thermites on a surface has been achieved in different morphologies: nanowires,[7–9] powders[10] and self-assembled nanorods or nanoparticles.[11,12] dc magnetron sputtering methods can also produce micro and nanostructured multilayered Al/CuO_x with different monolayer thicknesses. For example, Weihs and co-workers[13,14] studied combustion in micronized multilayered Al/CuO_x, Manesh *et al.*[15] have investigated the flame speed in sputter-deposited Al(26 nm)/CuO(54 nm) multilayered thermite on oxidized silicon substrates.

This paper presents a reactive magnetron sputter process designed to deposit microstructured and nanostructured multilayered Al/CuO reactive materials on a chip. The distinction between "microstructured" and "nanostructured" is set by the thickness of the Al or CuO monolayer: above 500 nm, the film is considered microstructured and below nanostructured. The dependence of the copper oxide composition on oxygen partial pressure and of the stress of multilayered thermites on the monolayer thickness was investigated. The heat of reaction of multilayered Al/CuO was then measured using differential scanning calorimetry (DSC) and differential thermal analysis (DTA). The contribution of this paper is twofold: first, we present a reactive magnetron sputter process to produce collectively high quality, pure and reproducible nanostructured Al/CuO thermite films that are completely compatible with MEMS device fabrication; second, we experimentally establish that reducing the individual Al and CuO monolayer thickness to 100 nm decreases the reaction temperature.

[a)]Electronic mail: mpetrant@laas.fr.

II. EXPERIMENTAL PROCEDURES

A. Samples preparation

Al/CuO samples were deposited on oxidized silicon wafers as multilayered thin films by the reactive magnetron sputtering technique. For thermal characterization, the silicon wafer was spin coated with a layer of photoresist prior to deposition, so that the Al/CuO multilayers could be easily peeled afterwards by dissolving the photoresist. The settings of the magnetron sputtering were optimized to minimize stress in the Al and CuO layers. The Al target (purity >99.999%) was dc sputtered under argon plasma at 800 W. The Cu target (purity>99.999%) was dc sputtered under argon and oxygen plasma at 400 W. Oxygen partial pressure was optimized at 0.13 Pa to obtain only CuO (see Sec. III). Then the equipment was programmed to sequentially deposit Al and CuO for a selected number of layers (see Table I). After the CuO layer deposition, the chamber was automatically pumped out to remove oxygen, thus preventing aluminum oxidation during the Al deposition cycle.

Selected thicknesses of Al and CuO layers have been processed, ranging from 25 nm to 1 μm, as summarized in Table II. For the thickest layers (1000 nm), deposition was done in 2 to 5 runs under pumping to avoid the target warm-up. After the sputter deposition of the Al/CuO multilayers, the silicon wafers with photoresist were placed in an acetone

TABLE I. Multilayered Al/CuO deposition parameters.

	Al	CuO
Target-substrate distance (cm)	8.5	8.5
Argon flow rate (SCCM)	50	100
Oxygen gas flow rate (SCCM)	0	25
Ultimate pressure (Pa)	2×10^{-5}	2×10^{-5}
Sputtering pressure (Pa)	1×10^{-1}	5×10^{-1}
dc power (W)	800	400
Substrate temperature (K)	283	283

bath and the Al/CuO multilayered films were peeled for thermal characterization. Then, samples were rinsed in an ethanol bath and dried. No thermal annealing was done at this stage.

B. Characterization methods

Structural microscopic characterization was performed by scanning and transmission electron microscopy (SEM and TEM, respectively). Roughness measurements were performed using atomic force microscopy (AFM). The multilayer composition was determined by x-ray diffraction (XRD) and Fourier-transform infrared spectroscopy (FTIR) analysis. Stress measurements were made by using a stylus profilometer. Thermal analyses were performed by DSC and DTA under nitrogen flow (purity of 99.999%) with a heating rate of 5 K/min. The temperature range varied from room temperature to 1000 K and 1473 K for DSC and DTA measurements, respectively.

III. RESULTS AND DISCUSSION

A. Sample structure and layers morphology: effect of oxygen on the sputter-deposited copper oxide films

The copper oxide layer was produced from a copper target under argon–oxygen plasma. The copper oxide composition obtained for 4 different oxygen partial pressures (0.05, 0.08, 0.10, and 0.13 Pa) was studied using XRD analysis.

For an oxygen partial pressure lower than 0.13 Pa, two types of copper oxides are produced: CuO and Cu_2O [see Figs. 1(a)–1(c)]. The heat released by the Al/Cu_2O thermite is almost half of that released by the Al/CuO thermite.[16] Therefore, CuO is better for our application requiring high energy release, and an oxygen partial pressure of 0.13 Pa was selected [see Fig. 1(d)]. In this case XRD analysis shows that

TABLE II. Multilayered Al/CuO samples.

Samples	Total thickness (μm)	CuO thickness (nm)	Al thickness (nm)	Surface layer
A	1.1	50	25	CuO
B	1.15	50	50	CuO
C	1	100	100	Al
D	1.1	100	100	CuO
E	2.1	100	100	CuO
F	2.1	1000	1000	CuO
G	3	1000	1000	CuO

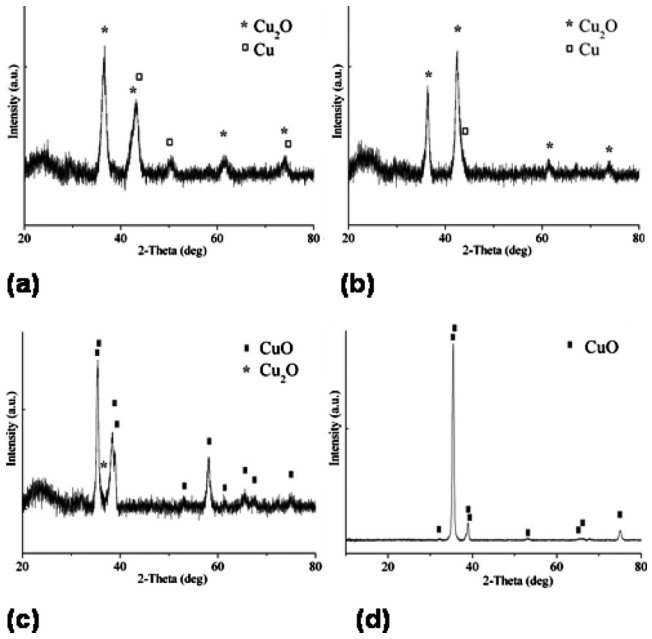

FIG. 1. XRD patterns of the CuO_x thin layers grown with oxygen partial pressures: (a) 0.05 Pa, (b) 0.08 Pa, (c) 0.10 Pa, and (d) 0.13 Pa.

the oxide is CuO. The FTIR absorption spectrum in Fig. 2 confirms the presence of copper (II) oxide, as evidenced by three bands at 507, 517, and 590 cm^{-1} characteristic of copper (II) oxide: CuO.[17] There is notably no evidence for copper (I) oxide, characterized by an absorption band at 623 cm^{-1}.[18] These results confirm that, above 0.13 Pa of oxygen, only CuO is formed.

Under these process conditions, the deposition rates of copper oxide and aluminum are 50 nm/min and 100 nm/min, respectively. For all samples, the thickness dispersion is measured to be lower than 5% for each individual monolayer. Samples with individual layer thickness (CuO or Al) lower than 100 nm are not stable: Al and CuO are found to react at ambient temperature and pressure during normal handling operations. For example, some of the B samples (see Table II) ignited spontaneously when nitrogen was introduced in

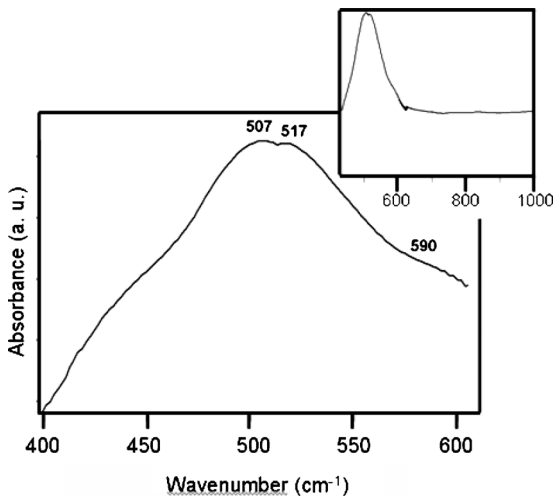

FIG. 2. Transmission infrared absorption spectra of magnetron sputtered CuO films (100 nm thick), using a blank Si substrate as reference. Inset: wider frequency range for the same sample.

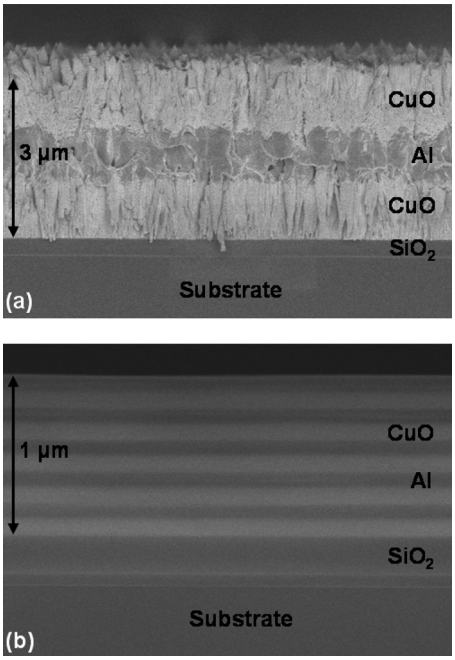

FIG. 3. SEM cross-section images of multilayers magnetron sputtered. A: 3 layers CuO(1 μm)/Al(1 μm)/CuO(1 μm). B: 10 layers of CuO(100 nm)/Al(100 nm).

the deposition device at the end of the deposition process. Furthermore, all the A-samples reacted spontaneously at in ambient conditions (in air at atmospheric pressure and temperature) without external stimuli. This observation suggest that the thin CuO or Al layers cannot prevent oxygen diffusion from the atmosphere, leading to the occurrence of hot (or ignition) points. Cross-section SEM images of the Al/CuO multilayered microstructured (G-type sample) and nanostructured (C-type sample) are shown in Figs. 3(a) and 3(b), respectively. The CuO layers morphology is clearly columnar (see Fig. 4). TEM analysis confirms the preferential orientation of the monoclinic CuO and the XRD analysis shows that this orientation is (11–1). AFM indicates a roughness of 1.2 nm and 2 nm for the CuO and Al thin layers, respectively.

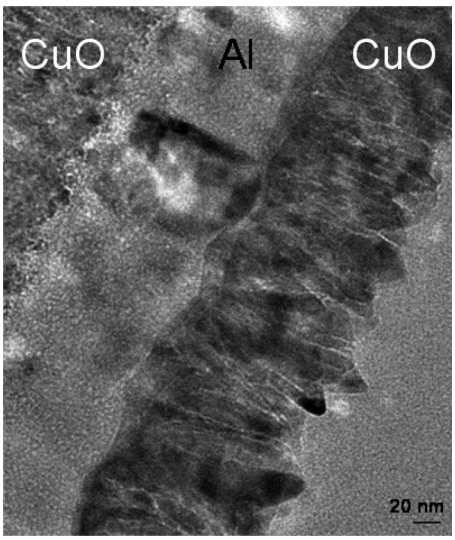

FIG. 4. TEM, cross-section image of multilayers magnetron sputtered Al/CuO.

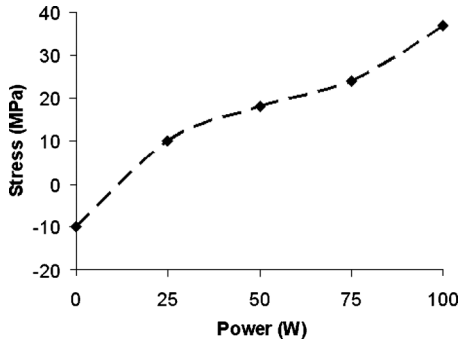

FIG. 5. Dependence of the stress in the thin aluminum layer on bias.

B. Stress measurement

The integration of these nanoenergetic layers into MEMS devices requires the formation of low-stressed layers to prevent cracking and peeling, which are often observed with Al/CuO nanowires producted by thermal treatment processes.[8]

Stress measurements were performed using a stylus profilometer: the wafer curvature was measured at the wafer surface before and after thin film deposition. The comparison between these two measurements gives the stress in the thin deposited film using the Stoney equation [Eq. (1)] (Ref. 19)

$$\sigma = \frac{1}{6K} \times \frac{E}{1-\upsilon} \times \frac{t_s^2}{t_f}, \tag{1}$$

where t_s and t_f are the wafer and film thicknesses, respectively; $[E/(1-\upsilon)]$ is the biaxial elastic modulus of the substrate [E: Young's modulus of the wafer (substrate) and υ: Poisson's ratio], and K is the variation in the wafer curvature.

The wafer diameter is cut in segments. On each segment, K is measured and the average of the stress value is obtained by determining the average of the K values.

The stress value depends of the deposition parameters, such as the gas pressure and the sputtering bias (substrate polarization during deposition), which have an impact on the density and porosity of the deposited layer. The argon flow rates were, therefore, optimized for the growth of both materials (Al and CuO) at 50 SCCM and 100 SCCM (SCCM denotes cubic centimeter per minute at STP), respectively, which gave a good tradeoff between deposition rate (50 nm/min and 100 nm/min, respectively) and thickness accuracy (5 nm). Furthermore, the CuO deposition parameters were optimized to obtain only the copper (II) oxide.

The stress in the CuO layer is about 33 MPa on a Si/SiO_2 substrate and about 32 MPa on a Si substrate. To minimize the multilayer stress during Al deposition, we varied the bias power. For instance, Al thin layers (100 nm) were obtained for five different values of the bias power: 0, 25, 50, 75, and 100 W. Figure 5 shows that the stress value increases with bias power. Without bias (power=0 W), a stress of -10 MPa is measured. For a bias power higher than 0 W, the stress becomes positive and increases with bias value (25–100 W) from 10 to 37 MPa. The resulting stress measured for multilayers is lower than 50 MPa, making these multilayered nanomaterials perfectly suitable for their integration into MEMS devices (see Table III).

TABLE III. Stress measurements results.

Samples	Stress measurement (MPa)
A	11
B	18
C	42
D	48
E	24
F	29
G	17

C. Reaction temperature and heat of reaction: microscale versus nanoscale

The DSC and DTA analyses of microstructured (F-type sample) and nanostructured (C-type sample) Al/CuO multilayers are shown in Figs. 6(a) and 6(b). The microstructured sample is characterized by two reaction steps, with an exothermic peak of ~0.7 kJ/g observed at ~790 K (onset temperature) and secondary exothermic peaks of 1.3 kJ/g above the aluminum melting point (between 1036 and 1356 K). The total heat of reaction is about 2 kJ/g. In contrast, the nanostructured layered sample features only a single exothermic reaction at ~740 K, that is far below the melting point of Al (933 K). The integration of this single exothermic peak area gives a heat of reaction of ~1.2 kJ/g, which is relatively low compared to the theoretical value (3.3 kJ/g) calculated for a reactant Al:CuO volume ratio of 1:1. The theoretical value is higher (3.9 kJ/g) for the stoichiometric conditions corresponding to a Al:CuO volume ratio of 1:1.8. A heat of reaction (1.8 kJ/g) lower than theoretically predicted (3.9 kJ/g) was also reported by Kim and Zachariah[20] for

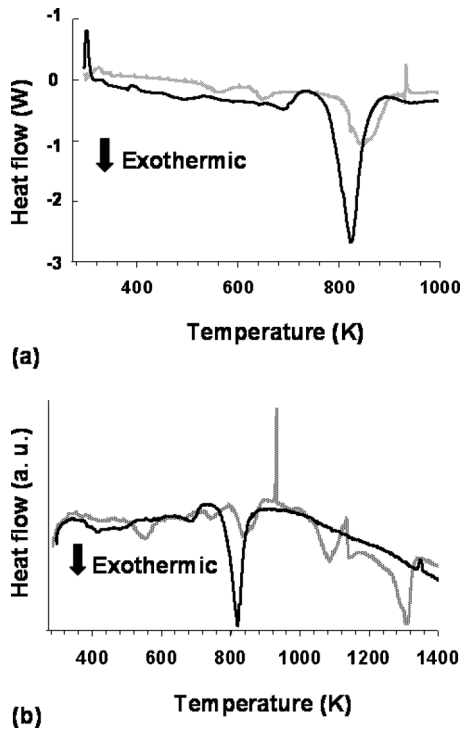

FIG. 6. Thermal analysis diagram for microstructured (gray curve) and nanostructured samples (black curve): (a) DSC and (b) DTA.

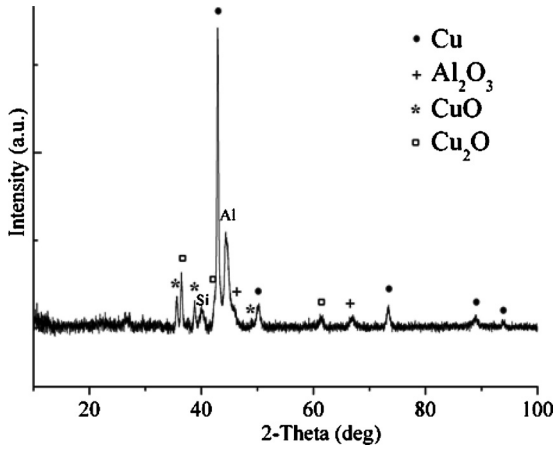

FIG. 7. XRD pattern of C-type samples after reaction in DSC.

Al/Fe_2O_3 nanoparticles. The discrepancy can be explained by the fact that the Al surface can be oxidized during the CuO deposition leading to an inert region, usually called interdiffusion zone between Al and CuO. Indeed, the Al surface is exposed to the $Ar-O_2$ plasma at the beginning of the CuO layer deposition, which is known to oxidize aluminum.

When Al and CuO layers thicknesses are below 100 nm, the thermite reaction occurs far below the melting point of Al. Thus these experiments indicate that the reaction involves a solid-solid atomic diffusion at the Al/CuO interface, although it is also possible that very thin Al layers can melt at temperatures lower than in a bulk state. In any case, the observation of only one exothermic reaction step at such low temperatures is unprecedented in the study of Al/CuO nanothermite. All previous investigations on multilayered thermites [with the individual layer thickness >500 nm (Refs. 7, 9, and 13) and (Ref. 14)] report the existence of two major peaks: one below and one above the Al melting temperature (~933 K).

XRD characterization of the residue of reaction (sample C-after DSC measurement) indicates that the final products of reaction are CuO, Cu_2O, Cu, and Al_2O_3 and maybe Al (see Fig. 7). The expected products of the reaction between Al and CuO are Cu and Al_2O_3. We find that there is also CuO and Cu_2O because the finely divided copper particles are readily oxidized in air. Despite Al oxidation during deposition, Al remains in excess in sample C because the reactants volume ratio is 1:1 while the stoichiometric ratio for Al/CuO is 1:1.8.

IV. CONCLUSIONS

Microstructured and nanostructured Al/CuO multilayers were deposited by dc reactive magnetron sputtering in argon–oxygen gas mixture plasma, with a thickness dispersion lower than 5% for each individual monolayer. This process is well adapted for the integration of nanoenergetic material into MEMS because it is versatile (multilayered film thickness is easily adapted) and can produce Al/CuO multilayered films with low stress (<50 MPa). This work also shows that multilayered Al/CuO films with monolayer thick-

nesses <100 nm can react spontaneously at ambient temperature (i.e., without thermal annealing) and are therefore unstable.

This study confirms that microstructured samples decompose in two-step reactions: a first exothermic reaction of ~ 0.7 kJ/g at ~ 790 K and a second exothermic reaction of 1.3 kJ/g between 1036 and 1356 K. It shows that, in contrast, there is only one exothermic reaction (~ 1.2 kJ/g) at lower temperature (about 740 K) for nanostructured films, well below the melting point of bulk aluminum (933 K).

In the future, we plan to develop a postprocessing step to stabilize Al/CuO surfaces and interfaces and to quantify the effect of the surface layer thickness and the interfaces on the heat release (ignition threshold and quantity of heat).

ACKNOWLEDGMENTS

We thank the French Military Agency (DGA) which has partially funded this work with a PhD grant and through one REI research project. The work was also possible through the PUF funding.

[1]K. Zhang, C. Rossi, M. Petrantoni, and N. Mauran, J. Microelectromech. Syst. **17**, 832 (2008).
[2]G. A. Ardila Rodríguez, S. Suhard, C. Rossi, D. Estève, P. Fau, S. Sabo-Etienne, A. F. Mingotaud, M. Mauzac, and B. Chaudret, J. Micromech. Microeng. **19**, 015006 (2009).
[3]H. Laucht, H. Bartuch, and D. Kovalev, Proceedings of the 7th International Symposium and Exhibition on Sophisticated Car Occupant Safety Systems, Karlsruhe, Germany, 12−16 November to December 1, 2004.
[4]D. S. Stewart, Proceedings of the 21st ICTAM, Warsaw, Poland, 15–21 August 2004.
[5]A. Bezmelnitsyn, R. Thiruvengadathan, S. Barizuddin, D. Tappmeyer, S. Apperson, K. Gangopadhyay, P. Redner, M. Donadio, D. Kapoor, S. Nicolich, and S. Gangopadhyay, Propellants, Explos., Pyrotech. **35**, 384 (2010).
[6]S. Gangopadhyay, R. Shende, S. Apperson, S. Bhattacharya, and Y. Gao, U. S. Patent No. 7608478 (27 October 2009).
[7]K. Zhang, C. Rossi, and G. A. Ardila Rodriguez, Appl. Phys. Lett. **91**, 113117 (2007).
[8]K. Zhang, C. Rossi, C. Tenailleau, P. Alphonse, and J. Y. Chane-Ching, Nanotechnology **18**, 275607 (2007).
[9]M. Petrantoni, C. Rossi, V. Conédéra, D. Bourrier, P. Alphonse, and C. Tenailleau, J. Phys. Chem. Solids **71**, 80 (2010).
[10]S. M. Umbrajkar, M. Schoenitz, and E. L. Dreizin, Thermochim. Acta **451**, 34 (2006).
[11]S. Apperson, R. V. Shende, S. Subramanian, D. Tappmeyer, and S. Gangopadhyay, Appl. Phys. Lett. **91**, 243109 (2007).
[12]J. Y. Malchi, T. Foley, and R. A. Yetter, ACS Appl. Mater. Interfaces **1**, 2420 (2009).
[13]K. J. Blobaum, M. E. Reiss, J. M. Plitzko, and T. P. Weihs, J. Appl. Phys. **94**, 2915 (2003).
[14]K. J. Blobaum, A. J. Wagner, J. M. Plitzko, D. Van Heerden, D. H. Fairbrother, and T. P. Weihs, J. Appl. Phys. **94**, 2923 (2003).
[15]N. A. Manesh, S. Basu, and R. Kumar, Combust. Flame **157**, 476 (2010).
[16]S. H. Fischer and M. C. Grubelich, Proceedings of the 24th International Pyrotechnics Seminar, Monterey, CA, 27–31 July 1998.
[17]A. Jagminas, J. Kuzmarskyte, and G. Niaura, Appl. Surf. Sci. **201**, 129 (2002).
[18]Y. C. Zhang, J. Y. Tang, G. L. Wang, M. Zhang, and X. Y. Hu, J. Cryst. Growth **294**, 278 (2006).
[19]G. Gerald Stoney, Proc. R. Soc. London, Ser. A **82**, 172 (1909).
[20]S. H. Kim and M. R. Zachariah, Adv. Mater.(Weinheim, Ger.) **16**, 1821 (2004).